ELSEVIER

Neuroscience Research 38 (2000) 63–70

Neuroscience Research

www.elsevier.com/locate/neures

Short communication

Difference in the metabolic response to photic stimulation of the lateral geniculate nucleus and the primary visual cortex of infants: a fMRI study

Tomoyo Morita[a], Takanori Kochiyama[a], Hiroki Yamada[b], Yukuo Konishi[c], Yoshiharu Yonekura[d], Michikazu Matsumura[a], Norihiro Sadato[e,*]

[a] *Graduate School of Human and Environmental Studies, Kyoto University, Kyoto, Japan*
[b] *Department of Radiology, Fukui Medical University, Fukui, Japan*
[c] *Department of Pediatrics, Fukui Medical University, Fukui, Japan*
[d] *Biomedical Imaging Research Center, Fukui Medical University, Fukui, Japan*
[e] *Department of Cerebral Research, Psychophysiology Section, National Institute for Physiological Sciences, Myodaiji, Okazaki, Aichi 444-8585, Japan*

Received 26 April 2000; accepted 26 May 2000

Abstract

The metabolic change that occurs during early development of the human brain was studied with functional magnetic resonance imaging (fMRI), in which the signal change reflects the balance between the supply and the demand of oxygen during stimulus-related neuronal activation. The subjects were 16 infants, aged < 1 year. They were sedated with pentobarbital, and 8-Hz flickering light was intermittently projected onto their eyelids. Two age groups were analyzed: infants < 60 days old and > 60 days old (corrected for gestational age at birth). The stimulus-related signal change was positive in the lateral geniculate nucleus regardless of the infants' age, but in the primary visual cortex reversed from positive in the younger group to negative in the older group. It is known that synaptogenesis in the lateral geniculate nucleus peaks before birth, and in the primary visual cortex accelerates in the second month after birth. Hence, the inversion of the stimulus-related signal change in the primary visual cortex may be due to an increased demand for oxygen owing to rapid synaptogenesis.

Keywords: Brain activation; Functional magnetic resonance imaging (fMRI); Infant; Lateral geniculate nucleus; Primary visual cortex; Synaptogenesis

1. Introduction

Functional magnetic resonance imaging (fMRI) is a noninvasive technique for mapping human brain function. The underlying mechanism of fMRI is the blood oxygenation level-dependent (BOLD) contrast arising from the paramagnetic property of deoxyhemoglobin (Pauling and Coryell, 1936), which influences the transverse relaxation rate of nuclear spins. In healthy adults, the BOLD effect is considered to be an indirect measure of the increase in regional cerebral blood flow (rCBF) caused by neuronal activation related to a task or stimulus. Increased neuronal activity leads to an increase in rCBF without a commensurate increase in oxygen extraction (Fox and Raichle, 1986). Hence, the capillary and venous deoxyhemoglobin concentrations decrease, which is reflected as an increase in the signal intensity of T2*-weighted MR images (Ogawa et al., 1990; Belliveau et al., 1991; Kwong et al., 1992; Ogawa et al., 1992). Studies on the sequence of events after neuronal activation suggest that the BOLD signal reflects transient oxygen consumption (Grinvald et al.,

* Corresponding author. Tel.: +81-564-557700; fax: +81-564-527913.
E-mail address: sadato@nips.ac.jp (N. Sadato).

0168-0102/00/$ - see front matter
PII: S0168-0102(00)00146-2

1991; Menon et al., 1995; Malonek and Grinvald, 1996; Hu et al., 1997). Before rCBF increases, the deoxyhemoglobin concentration following the onset of neuronal activation shows a small rise, lasting approximately 4 s and peaking at 2 s. This initial rise in deoxyhemoglobin is more localized to the site of neuronal activation and appears as a decrease in the BOLD signal (Menon et al., 1995; Hu et al., 1997). Hence, the BOLD signal change reflects the balance between the supply and the demand of oxygen during stimulus-related neuronal activation.

In early life, there is a rapid change in the anatomy, function, and metabolism of the human brain (Chi et al., 1977; Huttenlocher et al., 1982; Chugani and Phelps, 1986; Herschkowitz, 1988), which may be revealed by a change in the stimulus-related BOLD signal. fMRI studies of infants have shown that a signal change in the visual cortex in response to photic stimulation is the opposite of that in adults (Born et al., 1996; Yamada et al., 1997; Born et al., 1998). The change is positive before 8 weeks of age, but negative thereafter (Yamada et al., 1997). The abrupt change may be due to an increase in oxygen demand caused by rapid synapse formation and an accompanying increase in metabolism of the primary visual cortex (Yamada et al., 1997). If this is true, the neuronal substrates that have completed synapse formation before 8 weeks of age should show a positive response.

To test this hypothesis, we assessed the time-course of a stimulus-related BOLD signal change in the lateral geniculate nucleus (LGN) and primary visual cortex (V1). The LGN is an ideal 'control,' because it is the principal thalamic visual relay center linking the retina and the striate cortex, and its synaptogenesis is completed during the prenatal period (Wolff, 1981; Wadhwa et al., 1988; Khan et al., 1994). On the MRI, the stimulus-related signal increase in the LGN of adults (Büchel et al., 1997; Chen et al., 1998) is weaker than that of the V1, probably because of its small size (~ 5 mm). Therefore, we first located the LGN from its anatomical characteristics on a high-resolution structural MRI. This was followed by time-course analysis of the BOLD signal in the LGN and V1.

2. Subjects and methods

2.1. Subjects

We retrospectively reviewed the MRIs of 26 infants, aged < 1 year, whose prenatal exposure to high-risk conditions warranted MRI screening for possible brain damage. These subjects were involved in the fMRI protocol described by Yamada et al. (1997). The present data were obtained from February 1998 to February 1999, and therefore were not included in the earlier study (Yamada et al., 1997). Ten of the 26 MRIs were excluded because five showed anatomical abnormalities, and five others failed to detect the LGN due to technical difficulties. The remaining MRIs of 16 infants were analyzed. The infants' ages and high-risk conditions are summarized in Table 1. Follow-up revealed normal development. The Ethical Committee of Fukui Medical University approved the protocol, and written informed consent for the study was obtained from the infants' parents before the examination.

The experimental setup has been described by Yamada et al. (1997). In brief, the infants were sedated with pentobabital 3–5 mg/kg injected intravenously. The peripheral pulse rate and respiratory rate were

Table 1
Age and high-risk conditions[a]

Subject	Sex	Gestational age at birth (days)	Corrected age (days)	Chronological age (days)	Diagnosis
1	M	238	31	73	IRDS
2	M	215	33	98	IRDS
3	M	255	39	64	IUGR
4	F	201	42	121	IRDS
5	F	270	45	55	?Developmental delay
6	M	217	53	116	IRDS
7	F	196	55	139	IRDS
8	F	278	57	59	?CRS
9	F	280	94	94	IRDS
10	F	196	109	193	Premature (1152 g)
11	M	215	127	192	Premature (1410 g)
12	M	194	153	239	IRDS
13	M	272	178	186	?Congenital anomaly
14	M	216	273	337	IRDS
15	F	279	275	276	?Developmental delay
16	M	280	361	361	Asphyxia and hypoglycemia at birth

[a] Gestational age at birth was calculated from the mother's last menstrual period. Abbreviations: CRS, congenital rubella syndrome; IRDS, idiopathic respiratory distress syndrome; IUGR, intrauterine growth retardation.

monitored, and the infants were closely observed in the MRI unit. Their eyes were closed throughout the examination. A scanning session consisted of two rest periods and two stimulus periods, each 30 s long, with rest and stimulus alternating. An on–off cycle of 60 s was chosen to maximize the induced signal amplitude and to obtain a stable plateau of signal enhancement by the stimulus (Sadato et al., 1998). During the stimulus period, 8-Hz flickering light was projected onto the sedated infant's eyelids. During the rest period, the flickering light was turned off. The session was repeated twice. A time-course series of 42 volumes was acquired with a T2*-weighted, gradient echo echo-planar sequences with a 1.5 Tesla Signa Horizon MRI system (General Electric, Milwaukee, WI, USA) equipped with a standard birdcage coil. Each volume consisted of 12 contiguous horizontal slices 6–7 mm thick, including the calcarine fissure. The time interval between two successive acquisitions of the same slice (TR) was 3000 ms, and, hence, ten volumes were obtained in each rest and stimulus period. Echo time (TE) was 50 ms, and flip angle 90°. The field of view was 22 cm, and matrix size was 64×64, giving voxel dimensions of $3.4 \times 3.4 \times 6$–7 mm. Soon after the acquisition of all functional images was completed, structural T1-weighted images were collected in planes identical to the functional imaging slice (TR of 350 ms, TE of 15 ms, matrix size of 256×256, voxel dimensions of $0.86 \times 0.86 \times 6$–$7$ mm). All infants, sedated with pentobarbital, were confirmed no to move during the entire examination. And hence we assumed that both structural MRI and fMRI were obtained at exactly the same location.

2.2. Image and statistical analysis

The first two volumes of each fMRI scan were discarded because magnetization was unsteady, and the remaining 40 volumes were used for the analysis. The images from each subject were realigned with the last image as a reference by means of SPM96 software (Friston et al., 1995a) (Wellcome Department of Cognitive Neurology, London, UK) implemented in Matlab (Mathworks, Inc., Sherborn, MA, USA). Because the last functional image was obtained just before the structural image, these two images are considered to be collected in the same position. After the realignment, two-dimensional spatial smoothing with a Gaussian kernel of 4×4 mm was applied to each slice. Mean signal changes over the whole brain were removed by proportional scaling.

Due to poor myelination of infants' brain, structural MRI of infants provides poor contrast between the gray and white matter (Barkovich, et al. 1988), and hence direct visualization of the LGN is difficult. Despite of that, the T1-weighted structural MRI of infants can provide anatomical landmarks for identifying the LGN described by Horton et al. (1990). The LGN is found inferior to the lateral part of the posterior side of the pulvinar, and corresponds to the lateral portion of the ambient cistern (Horton et al., 1990). Because the horizontal section that crosses the superior colliculi and ambient cisterns includes the LGN (Horton et al., 1990), we first selected the appropriate transaxial slice of the structural MRI, and identified the LGN as an area capping the tip of the lateral recess of the ambient cistern (Fig. 1). Following the anatomical definition, the regions of interest (ROIs) of one pixel (3.4×3.4 mm) were placed on the LGN of both hemispheres. To confirm the feasibility of ROI on the LGN, we placed the 3×3 matrix of voxels around the voxel defined as the LGN, and calculated the stimulus-related increase of the BOLD signals. In all subjects, the center of the 3×3 matrix showed the maximal % increase of the signal intensity, and hence it may mainly represent the neural activity of the LGN.

Because the activation and deactivation patterns of the V1 elicited by a photic stimulus in infants varies anatomically, and, in particular, are distributed more anteriorly than in adults (Yamada et al., 1997; Born et al., 1998), we defined the ROI functionally. We assumed that the focus with the most significant stimulus-related signal change close to the calcarine sulcus represented the V1 of each subject. To locate the focus, we calculated the significance of the stimulus-related signal change on a voxel-by-voxel basis over the entire brain, using SPM99b software (Friston et al., 1994, 1995a,b). The general linear model was constructed with a stimulus-locked delayed box-car function (delay time, 6 s) as the effect of interest, and the low-frequency changes (by use of the discrete cosine basis function, with a cut-off period of 120 s) as the confound effect. On the assumption that the temporal autocorrelation was dominated by the hemodynamic response to neuronal activation, the time series data were smoothed with a Gaussian kernel of $\sqrt{8}$ s to enhance the signal relative to noise and to minimize bias in the estimate of error variance (Friston et al., 1994, 1995b; Worsley and Friston, 1995).

The question was whether the time series data covaried with the stimulus-locked delayed box-car function, and with statistical significance set at $P < 0.05$, corrected for multiple comparisons (Friston et al., 1995a), a statistical parametric map of the t statistic, SPM$\{t\}$ was constituted and superimposed on the structural MRI of each infant. We determined that the voxel of the local maximum in the SPM$\{t\}$ was located near the bank of the calcarine fissure bilaterally, and a ROI of 6.8×6.8 mm was placed on the local maximum point in each hemisphere (Fig. 1).

The time series of raw BOLD signals of the ROIs on the LGN and V1 obtained from the coregistered T2*-

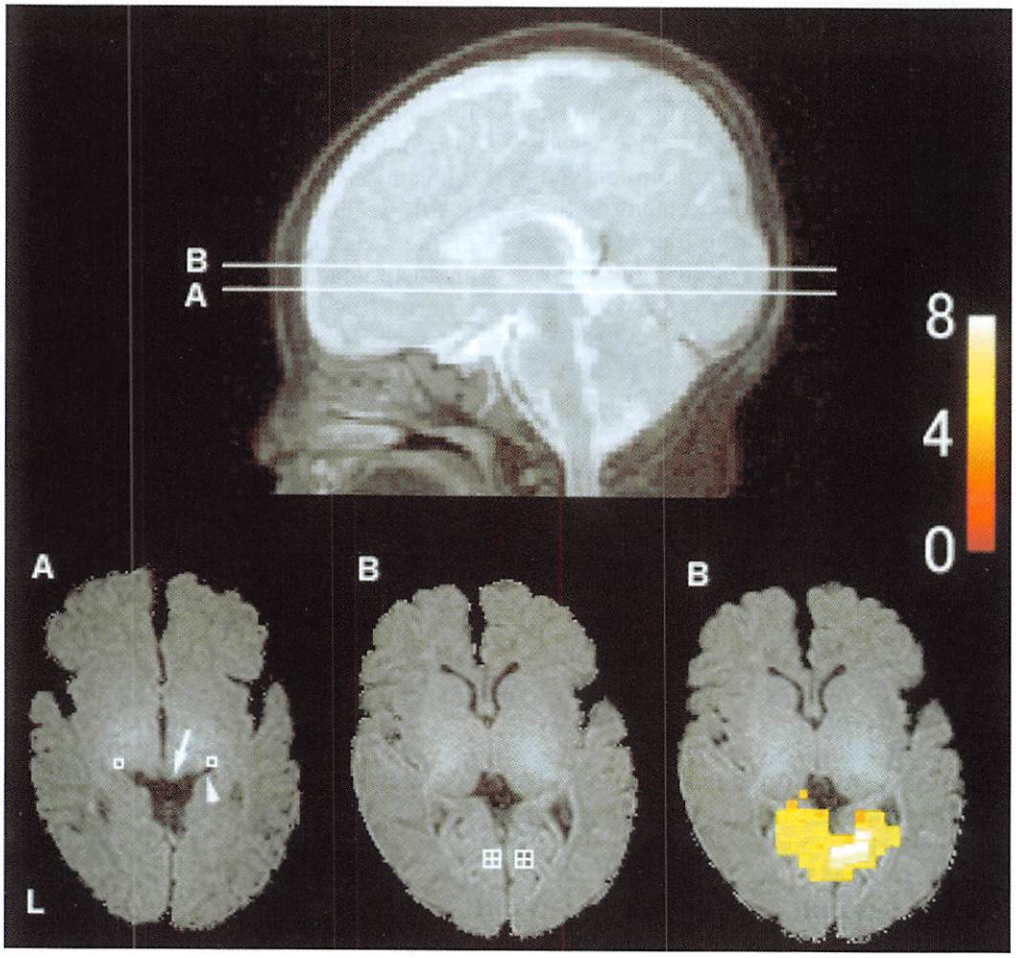

Fig. 1. Anatomical localization of the LGN and the V1 with T2-weighted sagittal view (top image) and T1-weighted transaxial view (bottom images) on the structural MRI from subject 1 aged 31 days (corrected) who showed positive signal response in the V1. (A) Transaxial view of the superior colliculus (arrow) and the ambient cistern (arrowhead). These structures, on which single-voxel ROIs (white squares) were placed, are the landmarks for identifying the LGN. (B) Transaxial view of the V1, parallel to and 7 mm above the superior colliculus. View on the right shows the statistical parametric map of the t statistic (SPM$\{t\}$) for comparison of the adjusted mean signal change in response to the photic stimulus versus that of the rest period superimposed on the MRI; the level of statistical significance is $P < 0.05$ (corrected). Note the anterior location of the activation pattern. The local maximum of the t statistic was localized, and four-voxel ROIs (white squares) were placed on each hemisphere (B, middle).

weighted echo planar images were analyzed with in-house software written by Matlab. Statistical analysis of the stimulus-related activation of the LGN and V1 was performed with a general linear model (Friston et al., 1994) similar to that based on SPM99b, described earlier. The time series data were smoothed with a Gaussian kernel of $\sqrt{8}$ s. The general linear model (Friston et al. 1994, 1995a,b) was constructed with the stimulus-locked delayed box-car function (delay time, 6 s) as the effect of interest, and the low-frequency changes (by use of a discrete cosine basis function with a cut-off period of 120 s) as the confound effect. Again, the question was whether the time series data covaried with the stimulus-locked delayed box-car function, and with statistical significance set at $P < 0.05$, the adjusted signals were obtained by removing the confound effect from the raw BOLD signals.

As in the previous study (Yamada et al., 1997), the subjects were divided into two age groups: younger (< 60 days of age, $n = 8$) and older (> 60 days of age, $n = 8$). The time course of the signal intensity from each ROI of each subject was converted to a percentage of signal change relative to the mean rest period signal, which was obtained by averaging the last eight time points of the two ten time-point rest periods of each session. The converted time courses were further averaged across two ROIs and two sessions for the V1 and LGN of each subject. The last eight time points of the ten time-point activation periods of the averaged time course of the percentage of signal change in the V1 were averaged to calculate the averaged stimulus-related percentage of signal change for each subject, allowing for random effect analysis. Similarly, the averaged percentage of signal change was calculated for the

LGN. In each age group, the statistical significance of the averaged stimulus-related percentage of signal change was evaluated by a two-tailed one-sample t test.

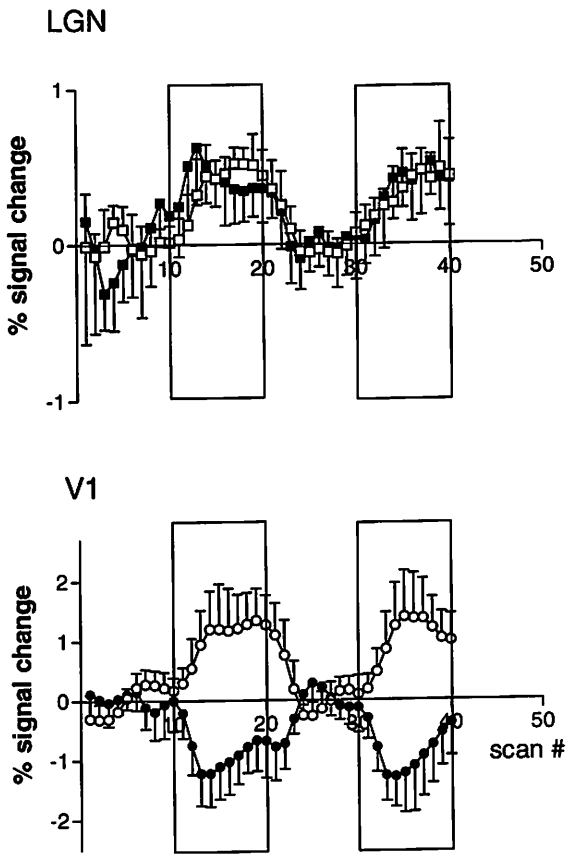

Fig. 2. Time courses of adjusted signal changes within each age group for the LGN and V1. The mean values at each scanning time point were obtained for the younger group (open symbols) and the older group (closed symbols), and were plotted the number of scan of 3-s interval. Error bars indicate the standard deviation ($n = 8$). Large rectangles represent the period of photic stimulation.

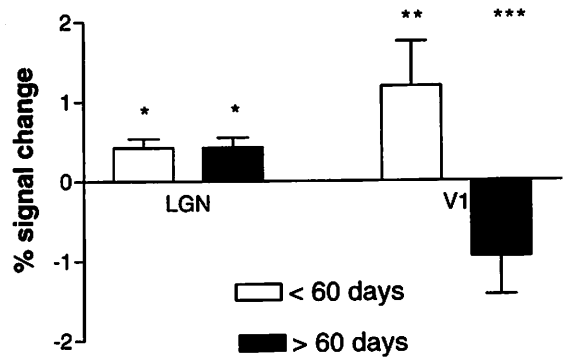

Fig. 3. Stimulus-related signal change (%) in the LGN and V1 of the younger group (age < 60 days, open bar, $n = 8$) and the older group (age > 60 day s, closed bar, $n = 8$). The change in the LGN was positive in both groups (*$P < 0.0001$, two-tailed one-sample t test), but in the V1 was positive in the younger group (**$P = 0.0005$) and negative in the older group (***$P = 0.001$).

3. Results

Age-related differences in the time course of the percentage of stimulus-related signal changes in the LGN and V1 are shown in Fig. 2. As shown in Fig. 3, the percentage of stimulus-related signal change in the LGN was positive regardless of the infants' age (younger group: $0.39 \pm 0.11\%$, $t(7) = 9.81$, $P < 0.0001$; older group: $0.37 \pm 0.09\%$, $t(7) = 11.78$, $P < 0.0001$). In the V1, however, the percentage of signal change was positive in infants younger than 60 days ($1.09 \pm 0.51\%$, $t(7) = 6.11$, $P = 0.0005$), but negative in older infants ($-0.83 \pm 0.44\%$, $t(7) = 5.38$, $P = 0.001$).

4. Discussion

We have shown that the time courses of the stimulus-related BOLD signal change in the V1 and LGN are different. As these structures are on the same visual pathway, it is conceivable that the neuronal activation of both increases during the stimulus. Hence, the difference in the time course can be attributed to a difference in the developmental course of these structures.

4.1. Primary visual cortex

Present study and previous report by Yamada et al. (1997) have shown that the V1 responses to the photic stimulation depends on the age corrected for genstational period. The signal response abruptly reversed from positive to negative at 8 weeks old, whereas marked overlap was noted if chronological age was adopted. This is due to the fact that subjects with perinatal risks which warranted the screening for MRI examination tended to be prematurely delivered, and hence chronological age usually surpasses the corrected age. This overlap suggests that the abrupt reversal of signal response reflects developmental processes which are not dependent of the period of visual exposure. Previous studies by Martin et al. (1999) and Born et al. (1998) adopted chronological age. Martin et al. (1999) included 58 subjects, describing a tendency of more frequent distribution of positive responses in younger age (< 4 months) than in elder groups, although it did not reach statistical significance. If corrected age had been applied, their results might have been different. Born et al. (1998) reported a study with smaller in size ($n = 11$), in which they did not observe positive response in the V1 in 11 subjects, four of them were younger than 6 weeks.

The V1, located mainly in the anterior portion of the calcarine sulcus, showed a stimulus-related signal decrease in infants older than 60 days of age and an increase in younger infants. This is concordant with the findings of other studies (Born et al., 1996; Yamada et al., 1997; Born et al., 1998; Martin et al., 1999). The

anterior activation may be partly due to an effect of the stimulus. Directing the photic stimulus to the subjects' eyelids would provide no spatial contrast, which may have caused greater activation in the peripheral retina than in the fovea and, thus, more anterior activation in the calcarine sulcus (Born et al., 1998).

Considering that the underlying mechanism of fMRI is the blood oxygenation level-dependent contrast arising from the paramagnetic property of deoxyhemoglobin (Ogawa et al., 1990), the stimulus-related decrease in the BOLD signal in the V1 of older infants is probably due to increased deoxyhemoglobin. The reversal of the stimulus-related MRI signal change may be explained by the dynamic morphological and metabolic changes of the V1 in early life. The V1 shows an exponential increase of synaptogenesis in the pre- and postnatal developmental periods both in nonhuman primates (Bourgeois and Rakic, 1993) and in humans (Huttenlocher et al., 1982). Positron emission tomography (PET) with ^{11}C-labeled glucose showed that cerebral glucose transport, as well as the glucose metabolic rate, is reduced in preterm human infants (Powers et al., 1998). PET with [^{18}F]fluorodeoxyglucose showed that the regional cerebral metabolic rate of glucose (rCMRGlc) of the whole brain correlates with postconceptional age up to 6 months (Kinnala et al., 1996). In infants 2 months of age and younger, CMRGlc is highest in the sensorimotor cortex, thalamus, and brain stem. By 3–5 months of age, CMRGlc has increased in the occipital cortex, as well as the frontal, parietal, temporal, and cerebellar cortical regions (Chugani and Phelps, 1986; Kinnala et al., 1996). As the rCMRGlc reflects synaptic activity (Raichle, 1987), an increase of CMRGlc in the visual cortex is compatible with the rapid synaptogenesis starting from the second month of age (Huttenlocher et al., 1982). The oxygen consumption of newborn humans is smaller than that of adults (Altman et al., 1993; Takahashi et al., 1999). PET with ^{15}O-labeled gas showed that the cerebral metabolic rate of oxygen ($CMRO_2$) in newborns who have minimal or no detectable brain injury is considerably below the threshold for brain viability in adults (Altman et al., 1993). This may indicate that the energy requirements of the fetal and newborn brain are minimal or can be met by nonoxidative metabolism. The rapid rise of $CMRO_2$ occurring from 1 to 3 years of age (Takahashi et al., 1999) suggests the developmental 'uncoupling' of glucose and oxygen metabolism, although studies simultaneously measuring the metabolism of glucose and oxygen in human infants are lacking.

Dynamic metabolic changes in the V1 in early life may explain the age-related reversal of the MRI signal. Because of rapid synapse formation, stimulus-related synaptic activity requires a larger amount of oxygen extraction than can be compensated by the rise in oxygen delivery from increased rCBF and cerebral blood volume. The resulting increase in deoxyhemoglobin concentration may cause reversal of the MRI signal (Yamada et al., 1997).

4.2. Lateral geniculate nucleus

In adults, the stimulus-related signal in the LGN is positive through the first year, with smaller incremental increases, compared with the V1 (Büchel et al., 1997; Chen et al., 1998). Unlike the V1, the LGN has completed the major portion of its developmental changes before birth. Most of the morphological and physiological changes in the LGN of prenatal humans are observed in the middle of the gestational period. At age 15–20 weeks there is a volumetric spurt (Khan et al., 1994). At 16–17 weeks, the number of optic axons from the retina to the LGN reaches a peak (Provis et al., 1985), and is accompanied by accelerated synaptogenesis in the LGN (Khan et al., 1994). At 17 weeks there is also a rapid increase in the gamma-aminobutyric acid (GABA) immunoreactive neuron (Wadhwa et al., 1988), which is a promoter of synaptogenesis (Wolff, 1981). Thereafter, the number of the axons decreases rapidly (Provis et al., 1985). In the later gestational period, the developmental change becomes stable, and by birth the morphological characteristics of the LGN resemble those of adults (Hitchcock and Hickey, 1980; Garey and de Courten, 1983; Provis et al., 1985; Khan et al., 1994). There are few reports on the developmental change in synapses in the LGN of humans during the postnatal period. After birth, the number of synapses in the LGN of the rhesus monkey does not exceed the birth level (Holstein et al., 1985). Considering that the LGN of both the rhesus monkey and the human shares similar morphological characteristics (Garey and de Courten, 1983) and developmental courses (Hitchcock and Hickey, 1980), the major portion of developmental change in the LGN of humans is likely to be complete before birth. Actually, in the rhesus monkey, neuronal projections from the two eyes become fully separated in the LGN subserving ocular dominance, but are only partially separated in the primary visual cortex 3 weeks before birth (Rakic, 1976). A positive stimulus-related signal change in the LGN through the first year, which is similar to the adult pattern, may reflect completion of maturation. This may explain relatively smaller variance of the stimulus related signal change in LGN than that of V1 (Fig. 3). Because of the dynamic synaptogenesis in V1 during early in life, stimulus related signal change in the V1 may vary across subjects within each early and late group. On the other hand, the synaptogenesis in the LGN has been already been completed. And hence its stimulus-related signal change varies less than that of V1.

4.3. Effect of sedation

Previous study by Martin et al. (1999) adopted three different regimens of sedation with different suppressive effects, which did show significant effect on the frequency distribution of positive/negative responses in the V1 of neonates. And hence the sedation is a confounding factor which should be controlled. Born et al. (1998) did not control the sedation effect: they treated nine subjects older than 4 weeks with chloral hydrate whereas two subjects younger than 6 days without sedation. Considering these previous results, present study adopted the identical regimen of sedation for all subjects with pentobarbital. Barbiturates act through the central nervous system, and nonanesthetic doses preferentially suppress polysynaptic responses. Facilitation is diminished, and inhibition is usually enhanced. The site of inhibition is postsynaptic in cortical cells and in the thalamic relay neurons. Enhancement of inhibition occurs primarily at synapses where neurotransmission is mediated by GABA acting at $GABA_A$ receptors (Hobbs et al., 1995). Hence, the effects of sedation on neural activity in the V1 and LGN are presumably similar. Furthermore, the protocol for sedation with pentobarbital was identical in all infants. For these reasons, the effect of sedation on the reversal of the BOLD signal would be minimal.

In conclusion, our results support the hypothesis that an abrupt change in the stimulus-related BOLD signal from positive to negative with aging in early life reflects an increased demand for oxygen owing to rapid synaptogenesis.

Acknowledgements

The authors are appreciative of the subjects' participation, and wish to thank the staff of the Biomedical Imaging Research Center, the Department of Radiology of Fukui Medical School for assistance with data collection, and B.J. Hessie, E.L.S., for skillful editing. This study was supported in part by a Research Grant (JSPS-RFTF97L00203) from the Japan Society for the Promotion of Science.

References

Altman, D.I., Perlman, J.M., Volpe, J.J., Powers, W.J., 1993. Cerebral oxygen metabolism in newborns. Pediatrics 92, 99–104.

Barkovich, A.J., Kjos, B.O., Jackson, D.E. Jr, Norman, D., 1988. Normal maturation of the neonatal and infant brain: MR imaging at 1.5 T. Radiology 166, 173–180.

Belliveau, J., Kennedy, D., McKinstry, R., et al., 1991. Functional mapping of the human visual cortex by magnetic resonance imaging. Science 254, 716–719.

Born, P., Rostrup, E., Leth, H., Peitersen, B., Lou, H.C., 1996. Change of visually induced cortical activation patterns during development. Lancet 347, 543.

Born, P., Leth, H., Miranda, M.J., et al., 1998. Visual activation in infants and young children studied by functional magnetic resonance imaging. Pediatr. Res. 44, 578–583.

Bourgeois, J.P., Rakic, P., 1993. Changes of synaptic density in the primary visual cortex of the macaque monkey from fetal to adult stage. J. Neurosci. 13, 2801–2820.

Büchel, C., Turner, R., Friston, K., 1997. Lateral geniculate activations can be detected using intersubject averaging and fMRI. Magn. Reson. Med. 38, 691–694.

Chen, W., Kato, T., Zhu, X.H., Strupp, J., Ogawa, S., Ugurbil, K., 1998. Mapping of lateral geniculate nucleus activation during visual stimulation in human brain using fMRI [published erratum appears in Magn. Reson. Med. 1998 Mar; 39(3):following 505]. Magn. Reson. Med. 39, 89–96.

Chi, J.G., Dooling, E.C., Gilles, F.H., 1977. Gyral development of the human brain. Ann. Neurol. 1, 86–93.

Chugani, H., Phelps, M., 1986. Maturation changes in cerebral function in infants determined by [^{18}F]FDG positron emission tomography. Science 231, 840–843.

Fox, P.T., Raichle, M.E., 1986. Focal physiological uncoupling of cerebral blood flow and oxidative metabolism during somatosensory stimulation in human subjects. Proc. Natl. Acad. Sci. USA 83, 1140–1144.

Friston, K.J., Jezzard, P., Turner, R., 1994. Analysis of functional MRI time-series. Hum. Brain Mapp. 1, 153–171.

Friston, K.J., Holmes, A.P., Worsley, K.J., Poline, J.B., Frith, C.D., Frackowiak, R.S.J., 1995a. Statistical parametric maps in functional imaging: a general linear approach. Hum. Brain Mapp. 2, 189–210.

Friston, K.J., Holmes, A.P., Poline, J.-B., et al., 1995b. Analysis of fMRI time-series revisited. Neuroimage 2, 45–53.

Garey, L.J., de Courten, C., 1983. Structural development of the lateral geniculate nucleus and visual cortex in monkey and man. Behav. Brain Res. 10, 3–13.

Grinvald, A., Frostig, R.D., Siegel, R.M., Bartfeld, E., 1991. High-resolution optical imaging of functional brain architecture in the awake monkey. Proc. Natl. Acad. Sci. USA 88, 11559–11563.

Herschkowitz, N., 1988. Brain development in the fetus, neonate and infant. Biol. Neonate 54, 1–19.

Hitchcock, P.F., Hickey, T.L., 1980. Prenatal development of the human lateral geniculate nucleus. J. Comp. Neurol. 194, 395–411.

Hobbs, W.R., Rall, T.W., Verdoorn, T.A., 1995. Hypnotics and sedatives; ethanol. In: Hardman, J.G., Goodman, G., Gilman, A., Limbird, L.E. (Eds.), Goodman & Gilman's The Pharmacological Basis of Therapeutics. McGraw-Hill, New York, pp. 361–396.

Holstein, G.R., Pasik, T., Pasik, P., Hamori, J., 1985. Early postnatal development of the monkey visual system. II: elimination of retinogeniculate synapses. Brain Res. 352, 15–31.

Horton, J.C., Landau, K., Maeder, P., Hoyt, W.F., 1990. Magnetic resonance imaging of the human lateral geniculate body. Arch. Neurol. 47, 1201–1206.

Hu, X., Le, T.H., Ugurbil, K., 1997. Evaluation of the early response in fMRI in individual subjects using short stimulus duration. Magn. Reson. Med. 37, 877–884.

Huttenlocher, P.R., de Courten, C., Garey, L.J., Van der Loos, H., 1982. Synaptogenesis in human visual cortex—evidence for synapse elimination during normal development. Neurosci. Lett. 33, 247–252.

Khan, A.A., Wadhwa, S., Bijlani, V., 1994. Development of human lateral geniculate nucleus: an electron microscopic study. Int. J. Dev. Neurosci. 12, 661–672.

Kinnala, A., Suhonen-Polvi, H., Aarimaa, T., et al., 1996. Cerebral metabolic rate for glucose during the first six months of life: an FDG positron emission tomography study. Arch. Dis. Child. Fetal Neonatal Ed. 74, F153–F157.

Kwong, K.K., Belliveau, J.W., Chesler, D.A., et al., 1992. Dynamic magnetic resonance imaging of human brain activity during primary sensory stimulation. Proc. Natl. Acad. Sci. USA 89, 5675–5679.

Malonek, D., Grinvald, A., 1996. Interactions between electrical activity and cortical microcirculation revealed by imaging spectroscopy: implications for functional brain mapping. Science 272, 551–554.

Martin, E., Joeri, P., Loenneker, T., et al., 1999. Visual processing in infants and children studied using functional MRI. Pediatr. Res. 46, 135–140.

Menon, R.S., Ogawa, S., Hu, X., Strupp, J.P., Anderson, P., Ugurbil, K., 1995. BOLD based functional MRI at 4 Tesla includes a capillary bed contribution: echo-planar imaging correlates with previous optical imaging using intrinsic signals. Magn. Reson. Med. 33, 453–459.

Ogawa, S., Lee, T.M., Kay, A.R., Tank, D.W., 1990. Brain magnetic resonance imaging with contrast dependent on blood oxygenation. Proc. Natl. Acad. Sci. USA 87, 9868–9872.

Ogawa, S., Tank, D.W., Menon, R., et al., 1992. Intrinsic signal changes accompnying sensory stimulation: functional brain mapping with magnetic resonance imaging. Proc. Natl. Acad. Sci. USA 89, 5951–5955.

Pauling, L., Coryell, C., 1936. The magnetic properties of and structure of hemoglobin, oxyhemoglobin and carbonmonoxyhemoglobin. Proc. Natl. Acad. Sci. USA 22, 210–216.

Powers, W.J., Rosenbaum, J.L., Dence, C.S., Markham, J., Videen, T.O., 1998. Cerebral glucose transport and metabolism in preterm human infants. J. Cereb. Blood Flow Metab. 18, 632–638.

Provis, J.M., van Driel, D., Billson, F.A., Russell, P., 1985. Human fetal optic nerve: overproduction and elimination of retinal axons during development. J. Comp. Neurol. 238, 92–100.

Raichle, M.E., 1987. Circulatory and metabolic correlates of brain function in normal humans. In: Mountcastle, V.M., Plum, F., Geiger, S.R. (Eds.), Handbook of Physiology. American Physiology Society, Bethesda, MD, pp. 643–674.

Rakic, P., 1976. Prenatal genesis of connections subserving ocular dominance in the rhesus monkey. Nature 261, 467–471.

Sadato, N., Yonekura, Y., Yamada, H., Nakamura, S., Waki, A., Ishii, Y., 1998. Activation patterns of covert word generation detected by functional MRI: comparison with 3D PET. J. Comput. Assist. Tomogr. 22, 945–952.

Takahashi, T., Shirane, R., Sato, S., Yoshimoto, T., 1999. Developmental changes of cerebral blood flow and oxygen metabolism in children. Am. J. Neuroradiol. 20, 917–922.

Wadhwa, S., Takacs, J., Bijlani, V., Hamori, J., 1988. Numerical estimates of GABA immunoreactive neurons in the human lateral geniculate nucleus in the prenatal period. Hum. Neurobiol. 6, 261–272.

Wolff, J.R., 1981. Evidence for a dual role of GABA as a synaptic transmitter and a promoter of synaptogenesis. Adv. Biochem. Psychopharmacol. 29, 459–465.

Worsley, K.J., Friston, K.J., 1995. Analysis of fMRI time-series revisited—again. Neuroimage 2, 173–181.

Yamada, H., Sadato, N., Konishi, Y., et al., 1997. A rapid brain metabolic change in infants detected by fMRI. Neuroreport 8, 3775–3778.